Supporting Information

Simultaneous synthesis of oxygen doped carbon electrodes at the anode and cathode *via* potential cycling for promoted H_2O_2 electrosynthesis

Suhua Mao [a], Xin Li [a,b], Bingshuang Li [a,c], Jin Li [a,c], Xiaoxi Huang [a,*]

[a] *Hoffmann Institute of Advanced Materials, Postdoctoral Innovation Practice Base, Shenzhen Polytechnic University, 7098 Liuxian Blvd, Nanshan District, Shenzhen 518055, P. R. China*

[b] *Key Laboratory of Plateau Oxygen and Living Environment of Tibet Autonomous Region, College of Science, Tibet University, Lhasa 850000, China*

[c] *Shenzhen Institute of Advanced Technology, Chinese Academy of Sciences, Shenzhen 518055, P. R. China*

Corresponding Author

**E-mail: xiaoxihuang@szpu.edu.cn*

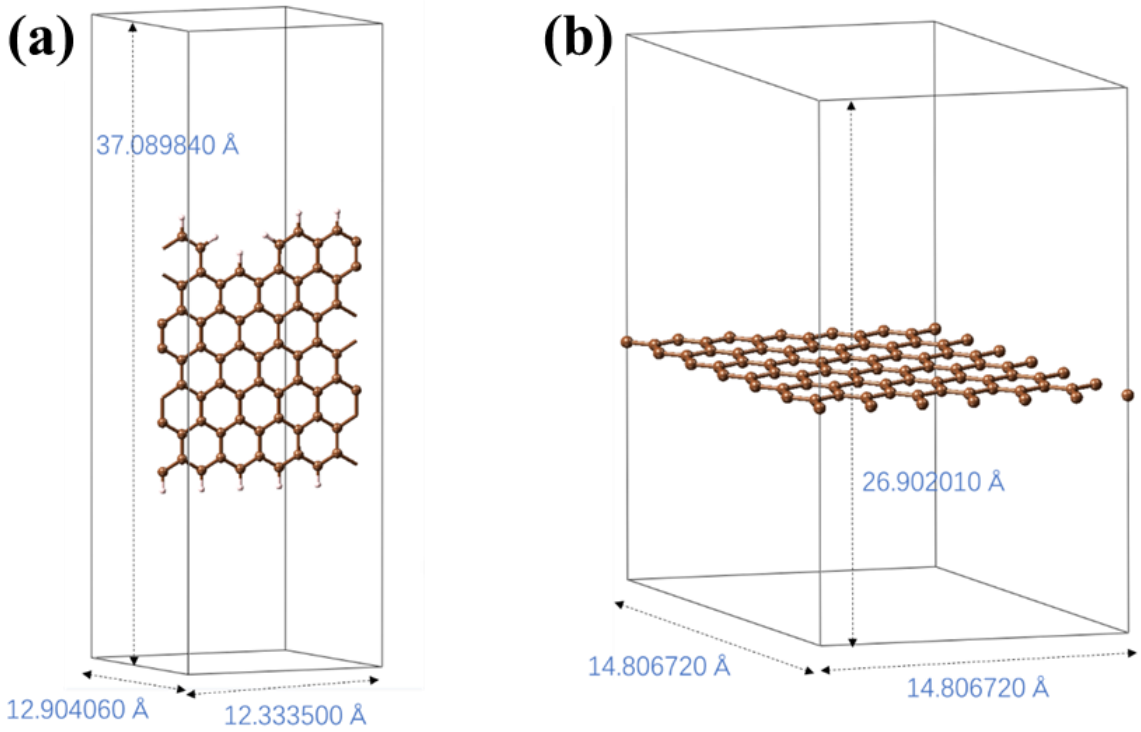

Figure S1. (a) The super cell of edge graphitic carbon without oxygen dopant, alpha = beta = gamma = 90°. (b) The super cell of basal graphitic carbon without oxygen dopant, alpha = beta = 90°, gamma = 120°. The other cell parameters are marked in the figure.

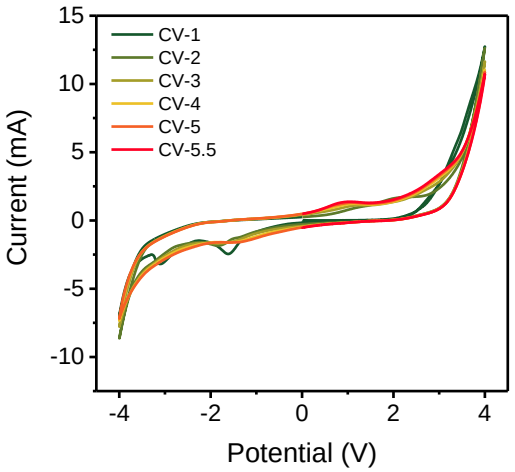

Figure S2. The recorded CV curves during electrochemical oxidation of carbon paper electrode.

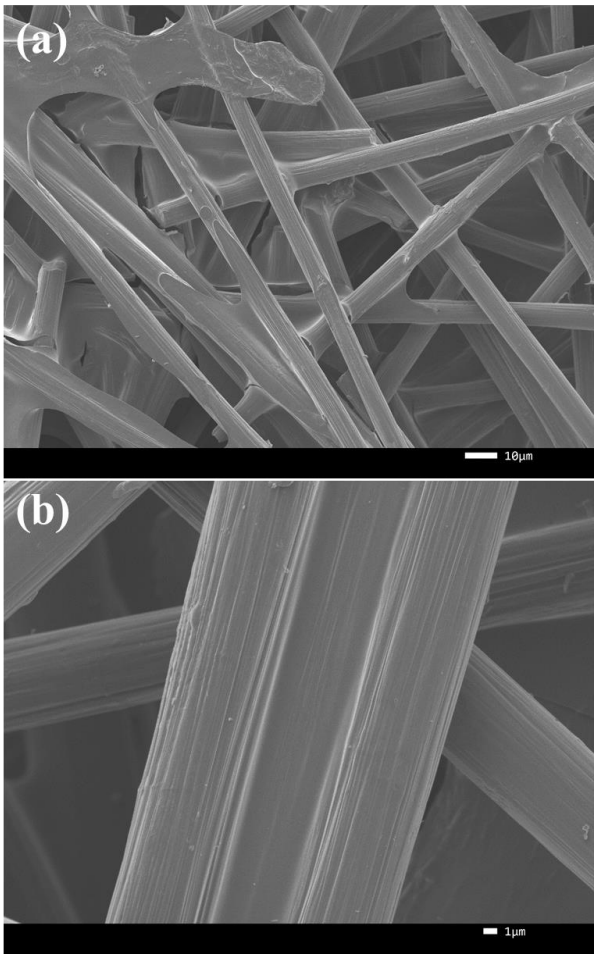

Figure S3. SEM images of original carbon paper (CP) at low magnification.

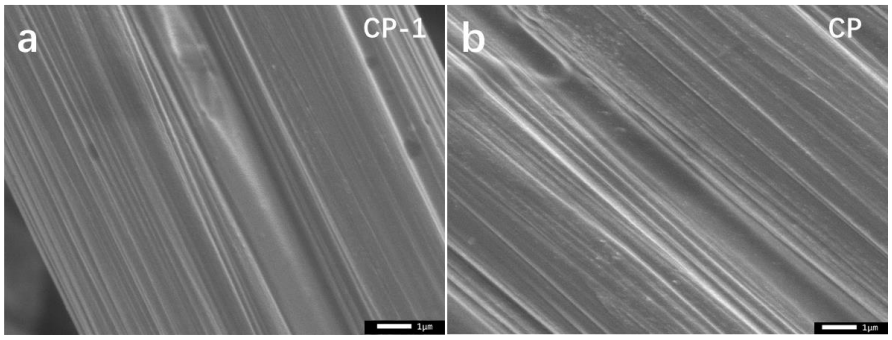

Figure S4. SEM images of CP-1 and CP at high magnification.

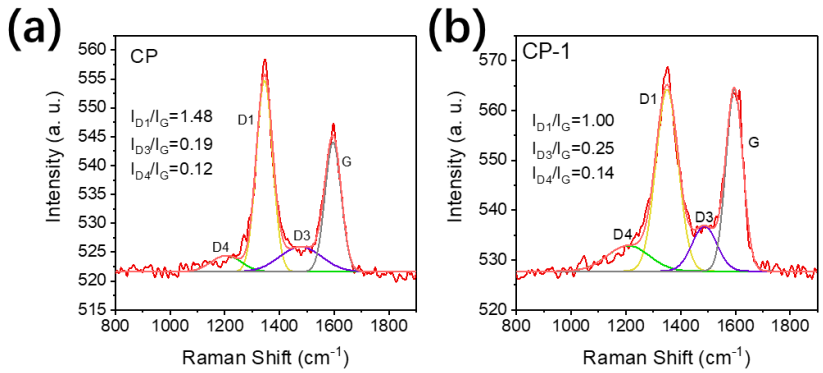

Figure S5. The Raman spectra of CP and CP-1.

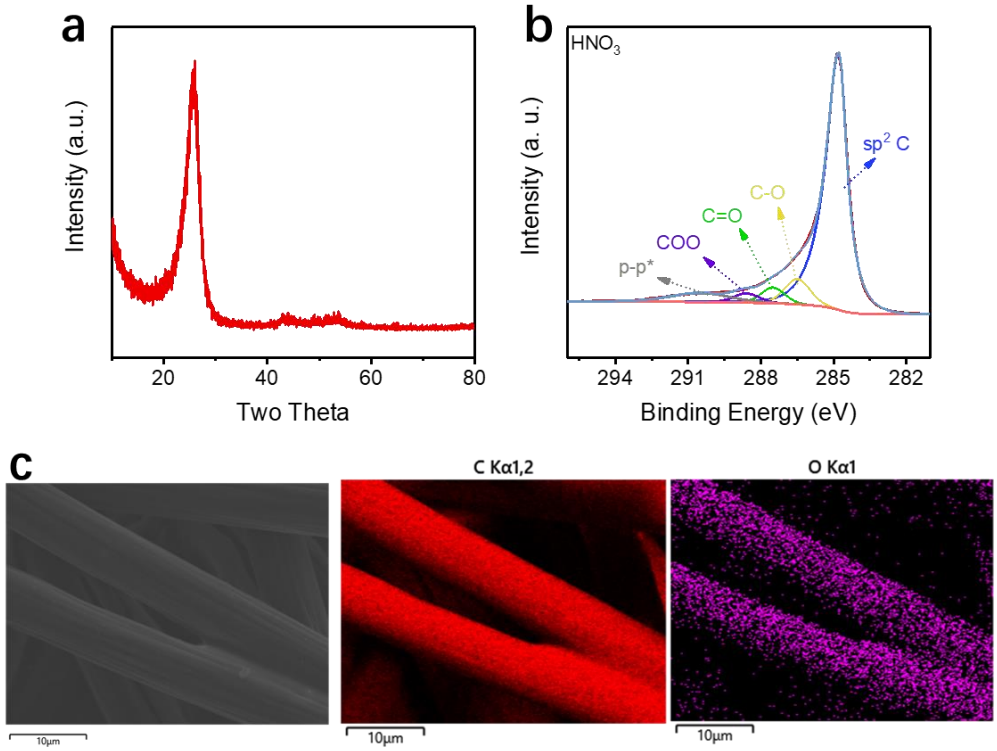

Figure S6. Physical characterization of carbon electrode oxidized by concentrated HNO_3. (a) XRD of CP-HNO_3. (b) Deconvolution of C 1s XPS spectra of CP-HNO_3. (c) Elemental mapping of carbon and oxygen, as well as corresponding electron microscope image for CP-HNO_3.

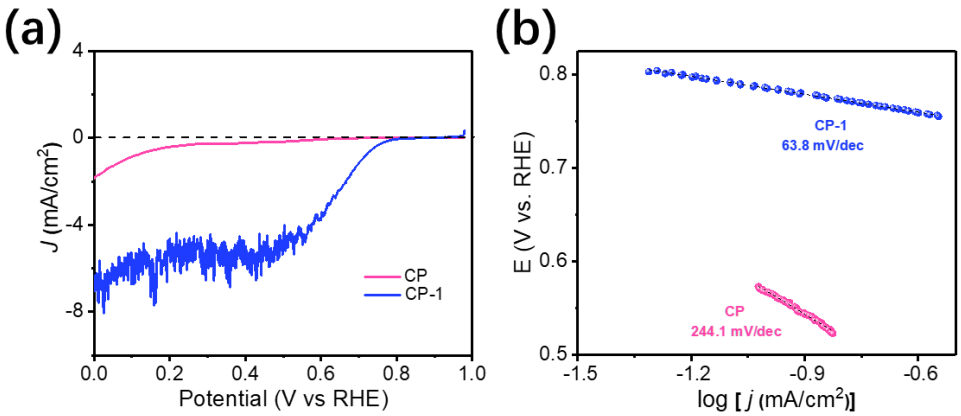

Figure S7. (a) Linear sweep voltammetry (LSV) curve of CP and CP-1 measured in oxygen saturated 0.1 M KOH solution. (b) Tafel plots derived from the LSV curves in (a).

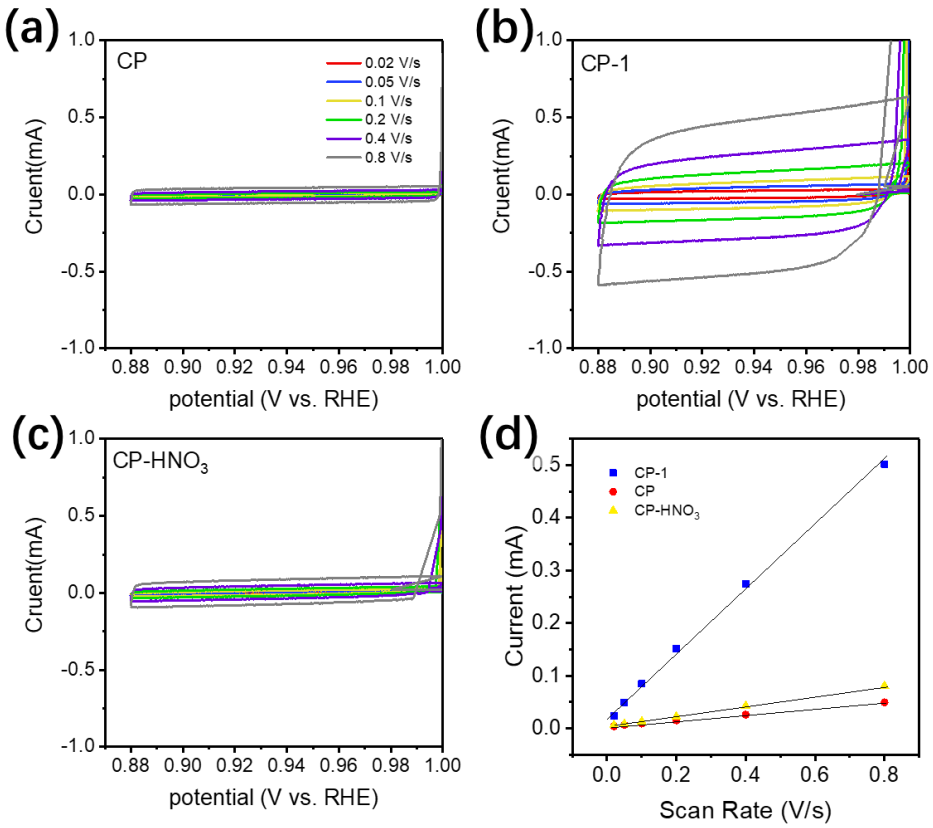

Figure S8. CV curves measured at a series of scan rates for (a) CP, (b) CP-1 and (c) CP-HNO_3 for the calculation of capacitance. (d) The plots of half of the difference between anodic current and cathodic current (0.94 V vs. RHE) versus the scan rates, the slope equals the capacitance of the electrode.

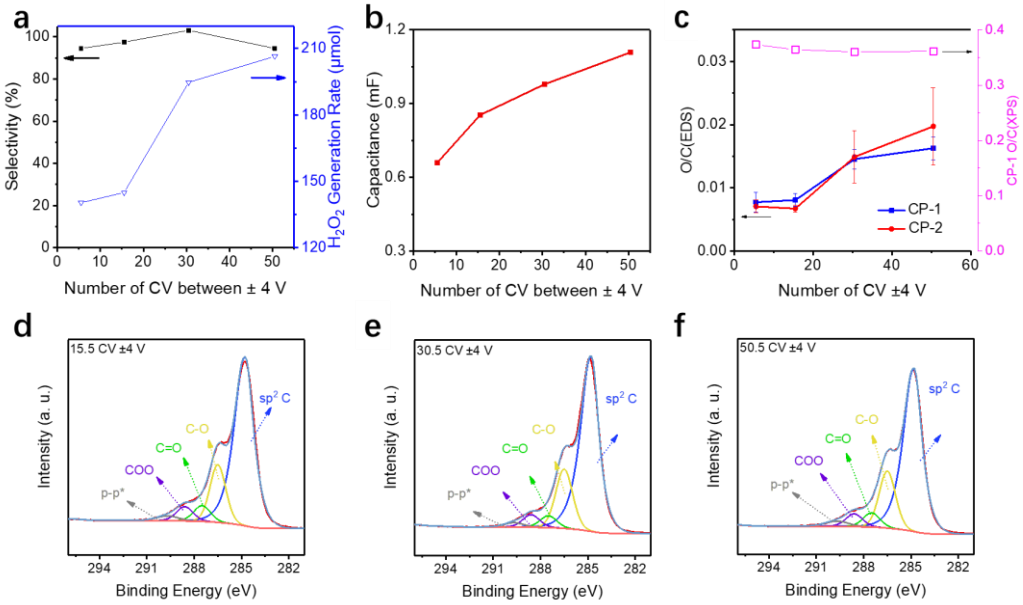

Figure S9. (a) H_2O_2 selectivity and generation rate catalyzed by carbon electrodes synthesized via different numbers of CV cycles between -4 V ~ +4 V, the ORR is evaluated at 0.38 V vs RHE. (b) The correlation between number of CV cycles and the capacitance of carbon electrodes. (c) The correlation between number of CV cycles and the ratios of O/C in carbon electrodes, both CP-1 and CP-2 data are included. The deconvolution of C 1s spectra for carbon electrodes synthesized by 15.5 (d), 30.5 (e) and 50.5 (f) cycles of CV.

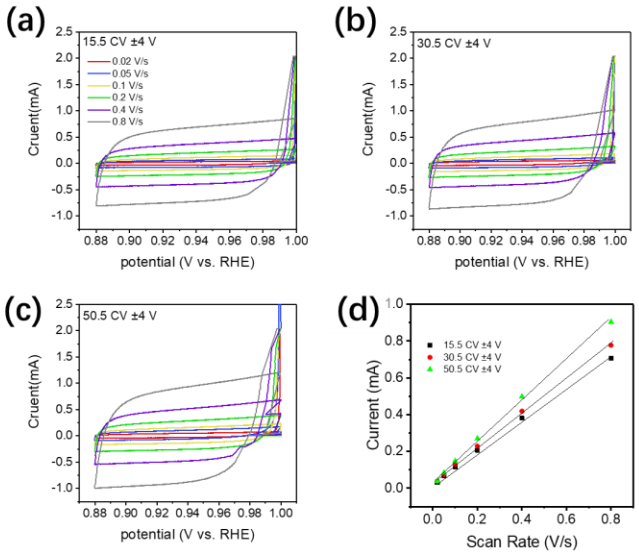

Figure S10. CV curves measured at a series of scan rates for carbon electrodes synthesized with (a) 15.5 cycles, (b) 30.5 cycles and (c) 50.5 cycles of CV. (d) The plots of half of the difference between anodic current and cathodic current (0.94 V vs. RHE) versus the scan rates, the slope equals the capacitance of the electrode.

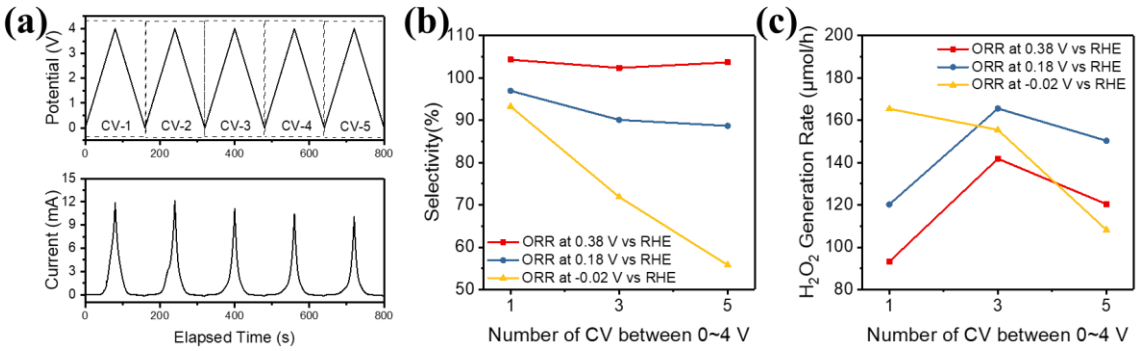

Figure S11. (a) The applied potential vs time and current vs time curves during electrochemical synthesis in the potential window of 0~4 V. (b) H_2O_2 selectivity and (c) generation rate in ORR catalyzed by CP electrodes oxidized between 0~4 V with one, three and five CV cycles.

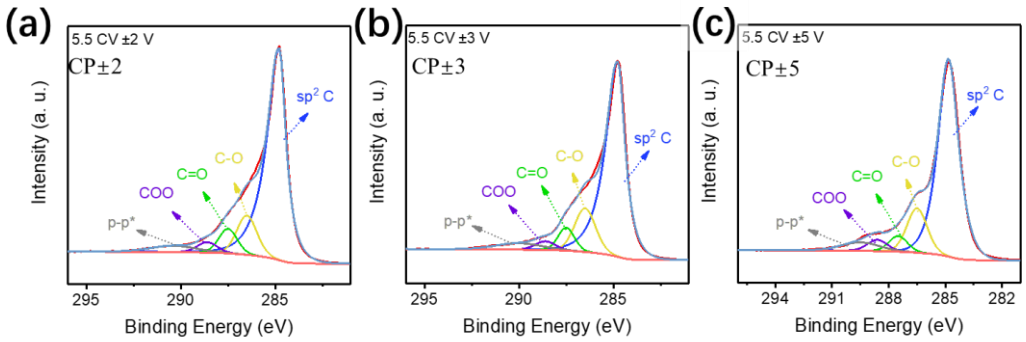

Figure S12. The deconvolution of C 1s spectra for carbon electrodes synthesized with 5.5 cycles of CV in the potential window of ±2 V(a), ±3 V(b), and ±5 V(c).

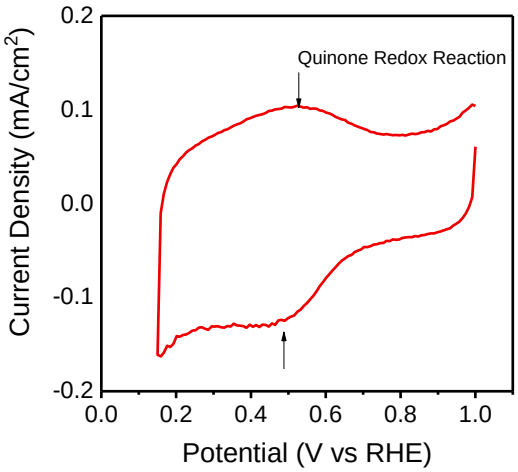

Figure S13. CV curve measured in Ar-saturated 0.5 M H_2SO_4 by using CP-1 (synthesized in the potential window of ± 4 V) at a scan rate of 50 mV/s.

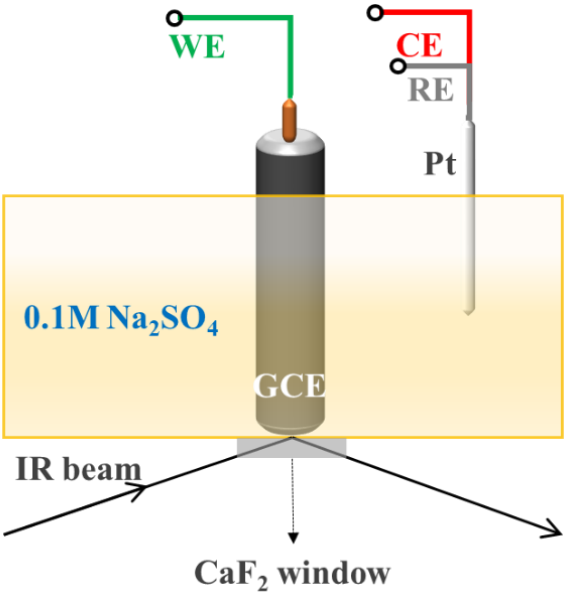

Figure S14. Schematic illustration of the setup for the Infrared test.

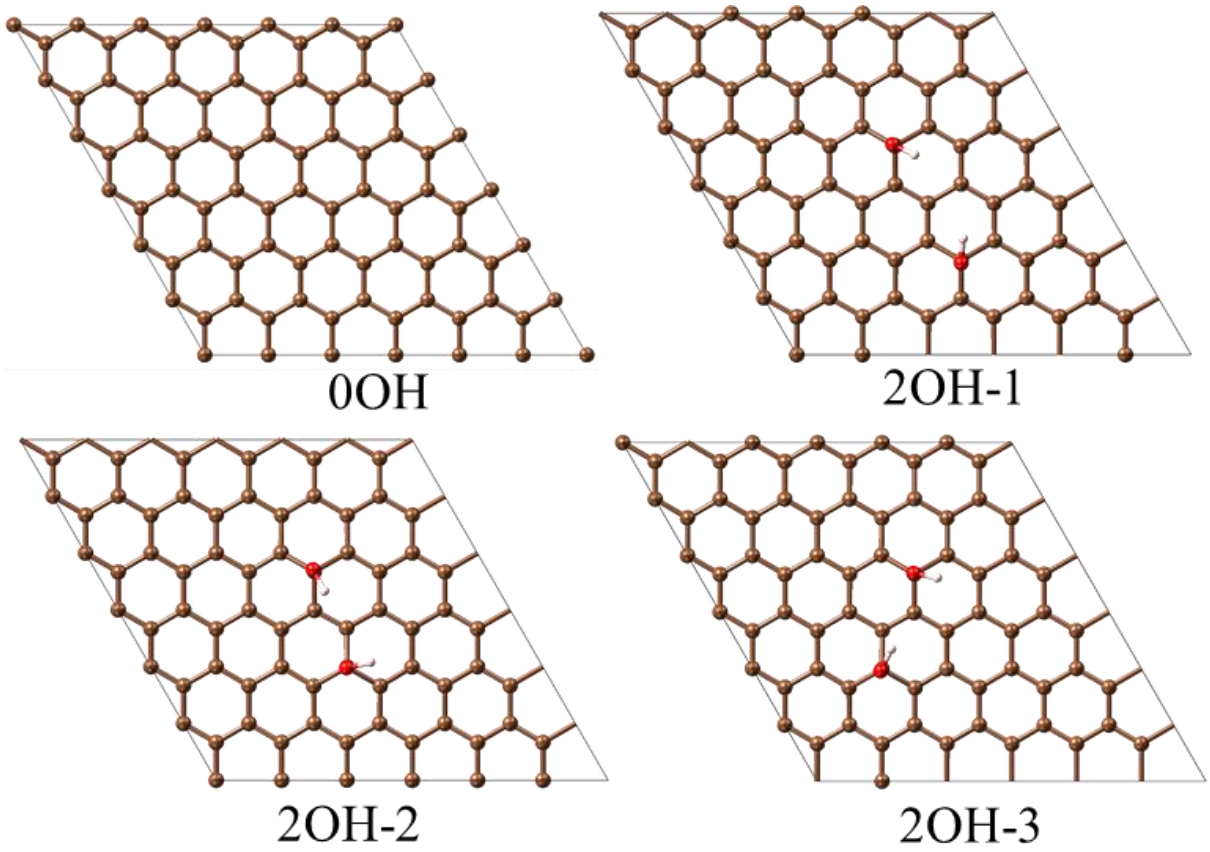

Figure S15. Catalyst slabs without hydroxyl group (0OH), and with two hydroxyl groups located different locations (2OH-1, 2OH-2, 2OH-3).

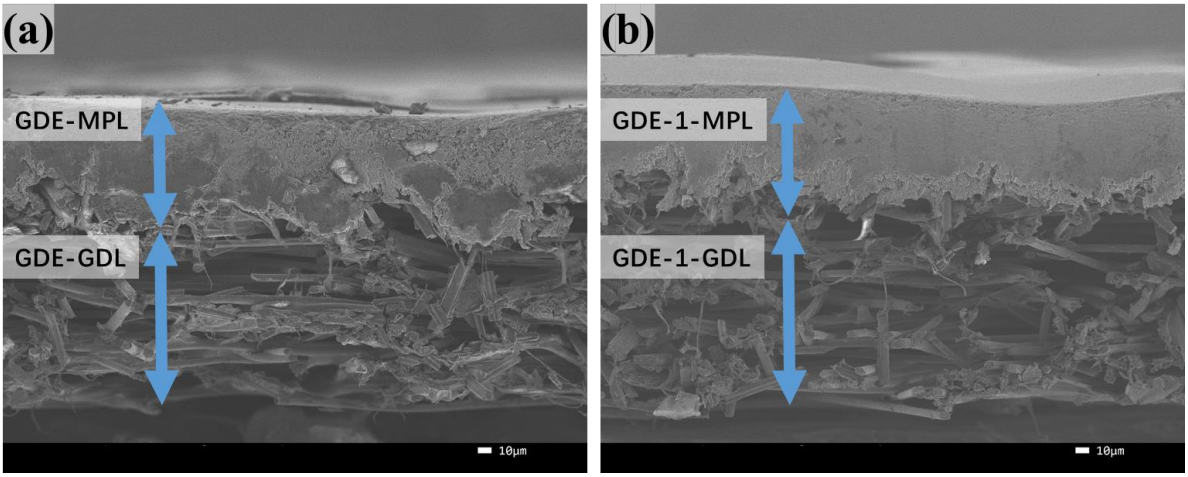

Figure S16. Cross-section SEM image of gas diffusion electrode before (GDE) and after (GDE-1) single side electrochemical oxidation.

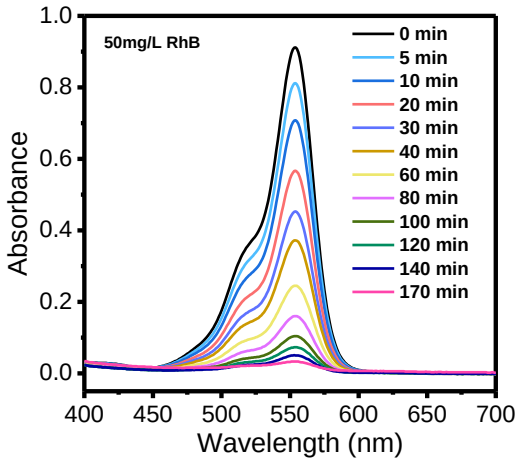

Figure S17. Time dependent UV-vis spectra of 50 mg/L RhB solution after mixing with electrolyte containing H_2O_2.

Table S1. Comparison of O_2 to H_2O_2 conversion performance of the electrodes in this work and previously reported materials in flow cell.

Catalyst	Electrolytes	Potential (V vs. RHE)	Selectivity	Current Density (mA/cm^2)	Ref.
GDE-1	1 M KOH	0.38	ca. 100%	300	This work
CoPc-CNT(O)	1 M Na_2SO_4	0.4	92%	300	[1]
CNT(O)	1 M Na_2SO_4	0.1	90%	200	[1]
Ni-SAC	1 M KOH	-2 V (cell voltage)	~91.4%	262	[2]
B/N-onion carbon	1 M KOH	0.6 (with iR compensation)	97.2%	400	[3]
B-C	1 M KOH	0.685 (with iR compensation)	85.1%	300	[4]
PANI/CDs-Co-2	0.1 M KOH	0	86.5%	85	[5]
$MHCS_{0.5}$	0.1 M KOH	0.1	ca. 90%	254	[6]
MeCN	0.1 M KOH	0.2	> 95%	202	[7]
NBO-G/CNTs	0.1 M KOH	-0.5	--	100	[8]

Reference

1. B.-H. Lee, H. Shin, A. S. Rasouli, H. Choubisa, P. Ou, R. Dorakhan, I. Grigioni, G. Lee, E. Shirzadi, R. K. Miao, J. Wicks, S. Park, H. S. Lee, J. Zhang, Y. Chen, Z. Chen, D. Sinton, T. Hyeon, Y.-E. Sung and E. H. Sargent, *Nat. Catal.*, 2023, **6**, 234-243.
2. Y. Sun, K. Fan, J. Li, L. Wang, Y. Yang, Z. Li, M. Shao and X. Duan, *Nat. Commun.*, 2024, **15**, 6098.
3. J. Qi, Y. Du, Q. Yang, N. Jiang, J. Li, Y. Ma, Y. Ma, X. Zhao and J. Qiu, *Nat. Commun.*, 2023, **14**, 6263.
4. Y. Xia, X. Zhao, C. Xia, Z. Y. Wu, P. Zhu, J. Y. T. Kim, X. Bai, G. Gao, Y. Hu, J. Zhong, Y. Liu and H. Wang, *Nat. Commun.*, 2021, **12**, 4225.
5. Y. Zhou, X. Gu, J. Wu, H. Huang, M. Shao, Y. Liu and Z. Kang, *Appl. Catal. B Environ.*, 2023, **322**, 122105.
6. Q. Tian, L. Jing, H. Du, Y. Yin, X. Cheng, J. Xu, J. Chen, Z. Liu, J. Wan, J. Liu and J. Yang, *Nat. Commun.*, 2024, **15**, 983.
7. Q. Tian, L. Jing, Y. Yin, Z. Liang, H. Du, L. Yang, X. Cheng, D. Zuo, C. Tang, Z. Liu, J. Liu, J. Wan and J. Yang, *Nano Lett.*, 2024, **24**, 1650-1659.
8. M. Fan, Z. Wang, K. Sun, A. Wang, Y. Zhao, Q. Yuan, R. Wang, J. Raj, J. Wu, J. Jiang and L. Wang, *Adv. Mater.*, 2023, **35**, e2209086.